Journal of Visualization, Vol. 5, No.1 (2002) 51-57

Stereoscopic PIV Measurements of Flow in and around Axial Flow Fan

Yu-Cheong, I.*1, Kobayashi, T.*1, Saga, T.*1 and Itoh, T.*2

*1 Institute of Industrial Science, The University of Tokyo, 4-6-1 Komaba, Meguro-Ku, Tokyo 153-8505, Japan.
*2 Tsuruoka Higashi Plant, 3-4-10 Takarada, Tsuruoka-shi, Yamagata 997-0011, Japan.

Received 2 August 2001.
Revised 29 October 2001.

Abstract: To analyze the complex three-dimensional flow structure of an axial flow fan and determine the validity of its application, PIV is used to provide detailed space and time resolved experimental data for understanding and control of flow field. The high resolution stereoscopic PIV system was successfully employed in this study for the investigation of flow structure around the axial flow fan. Using the once-per-revolution signal from the rotor, image fields were captured at a fixed position of the blades and hence provides the ability to do phase-averaging. The three-dimensional instantaneous velocity fields, phase-averaged velocity fields, instantaneous and mean vorticity distributions of the stereoscopic PIV measurement results were represented at typical planes of the flow field. Phase-averaged velocity fields were calculated based on 200 frames of the instantaneous stereoscopic PIV measurement results. From the velocity distribution, the vorticity and turbulent intensity distribution, which are known to be major factors of fan noise, were calculated and its diffusion was discussed as they travel downstream. From the reconstructed three-dimensional velocity iso-surface at 8 cross planes of the outlet flow fields, the three-dimensional features can be seen clearly.

Keywords: stereoscopic PIV technique, axial flow fan, once-per-revolution signal, velocity iso-surface.

1. Introduction

In connection to the development of fluid machinery such as aircraft and vehicle dynamics the investigation of air flows has been motivated to improve the system performance in these years. Especially, the axial flow fan is widely used for industrial equipment and household appliances such as air-conditioner. Considerable efforts have been made to investigate transient events of axial flow fan in depth with developments in the vehicle and aircraft industries. The design of axial flow fan, however, has not yet been well established because of the complexity of the internal inflow and outflow (turbulence near the suction side of blade, vortex shedding and inflow and outflow) which is a major contributor to a source of noise. To improve the system performance and reduce the noise from that part, it is important to get further information on the flow pattern around the axial flow fan.

Although a variety of experimental and theoretical approaches (Rajan et al., 1998 and Sharland, 1964) has been conducted in previous studies, much work is still needed in order to examine the detailed flow property in and around the axial flow fan, especially in relation to the mechanisms of vortical and turbulent flow from the blades and its diffusion to the downstream. To analyze increasingly complex three-dimensional flow structure of the axial flow fan and to determine the validity of its application, conventional two-dimensional measurement result (Adrian, 1991) would not allow insight into the nature of the three-dimensional flow.

In order to reveal the three-dimensional features of the axial flow fan, high-resolution stereoscopic PIV (Saga, 1999), which can obtain all the three components of the velocity vector simultaneously, is used in this study to measure the flow field of axial flow fan. Stereoscopic PIV technique, using two cameras viewing the flow from

two perspectives, is good for visualization and for the measurement of the three velocity components in the illuminating laser sheet plane. By reconstructing the vector fields from the two cameras, the three-dimensional velocity field in the objective plane was measured. Based on the three measurement results of the stereoscopic PIV system, three component velocity fields and the vorticity distribution were represented.

2. Experimental Apparatus and Setup

Figure 1 represents a measuring region in geometric configuration of an axial flow fan. The test fan named "windward tilted blade fan" has 5 blades with an angle attack of 18 degrees. The blade tip to tip diameter and the hub diameter are 174 mm and 80 mm (tip clearance: 3 mm, hub to tip ratio: 0.45) respectively and the width of the test fan is 90mm. The rotational speed of the impeller is maintained at 2500 rpm. A test fan was mounted on a two-dimensional movable table so that the distance between illuminating laser sheets and the different cross planes can be changed by sliding the two-dimensional movable table mechanism. On those arrangements, the size of common measurement region of the two image recording cameras is about 100 mm by 100 mm. It can be seen that the region of measurement covered 25% of the flow field in the rotor exit region. At each location (1 inlet, 2 internal and 8 outlet) 200 images were obtained in the phase-locked mode.

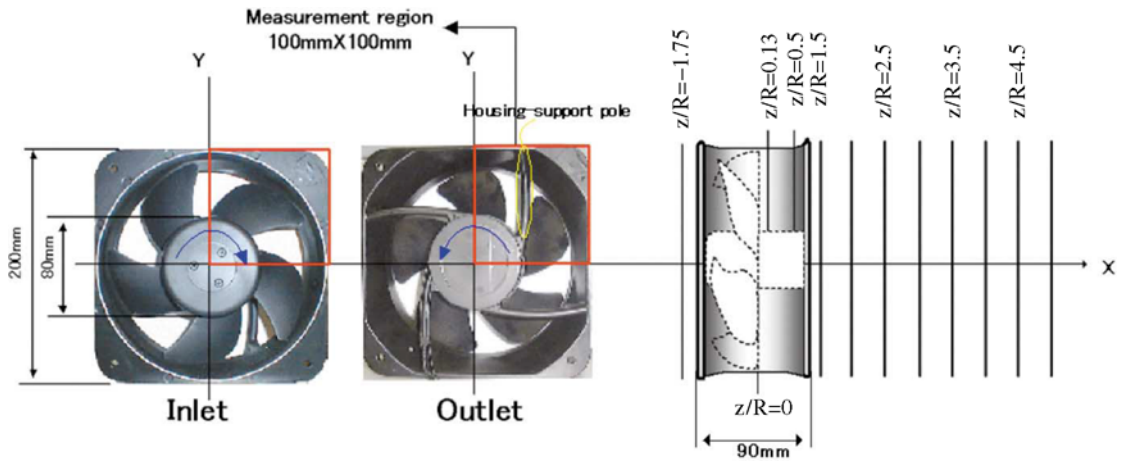

Fig. 1. Schematic diagram of axial fan.

Figure 2 represents the schematic of the experimental setup used in this study. A pair of cameras and the laser light assembly were mounted on the same fixture to obtain the image field in the x-y plane at various z-axis locations. For illuminating the flow field, a double pulsed Nd:YAG lasers (pulsed illumination duration of 6 ns) with the frequency of 15 Hz and power of 20 mJ/pulse were used. The combined beam from the two laser tubes was delivered to the measuring region using the various optics. The optics installed in a laser head unit provides a laser sheet (thickness of about 2.0 mm), whose thickness and angle of divergence could be controlled. DEHS (Di-2-Ethlhexyl-Sebact) droplets were used as tracer particles with diameter of 1 μm. Those tiny particles were generated by a seeding generator that is composed by an air compressor and several Laskin nozzles. To capture the flow field simultaneously with high resolution, a pair of cross-correlation CCD cameras (TSI PIVCAgM 10-30) with 1000 by 1016 pixels resolution was used. In order to have the measurement field focused on the image planes perfectly, tilt-axis mounts were installed between the camera bodies and lenses. The distance between the illuminating laser and image recording plane of the cameras are about 720 mm and the angle of between the view axis of the two cameras is about 50°. Cameras and laser were connected to a workstation (host computer) via synchronizer (TSI Laser Pulse synchronizer), which controlled the timing of the laser sheet illumination and the CCD camera data acquisition. In the present study, the time interval between the two laser pulses were settled as 22 μs~30 μs at various z-axis locations. The high speed host computer allows stereoscopic PIV image pairs to be captured for up to 250 frames at the framing frequency of 15 Hz. A once-per-revolution signal from the rotor (encoder system was attached to the rotor) was also used as the input to the synchronizer so that phase-locked image capture could be accomplished. This allows the flow fields to be acquired at a fixed position of the blades and hence provides the ability to do phase-averaging.

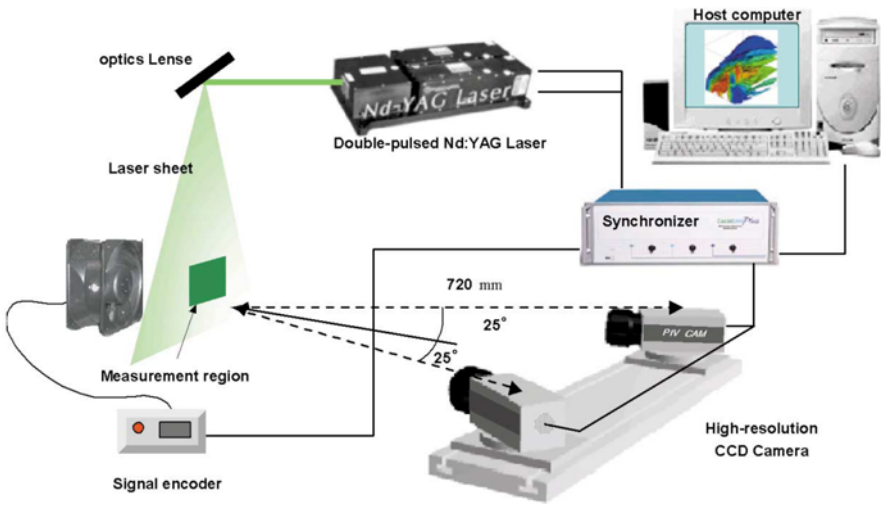

Fig. 2. Schematic arrangement of PIV system.

3. Experimental Results

By using the two-dimensional particle image displacement detected by left and right image recording cameras, the three-dimensional displacement vectors in the physical space of the objective fluid flow were reconstructed by solving Eq. (1) . In this Eq. (1), the four terms $\Delta X_1^{(1)}$, $\Delta X_2^{(1)}$, $\Delta X_1^{(2)}$, $\Delta X_2^{(2)}$ in the left side are the image plane displacement on the left and right image recording planes. The 12 terms in the transformation matrix (∇F) are the derivatives of the general mapping function.

$$\begin{pmatrix} \Delta x_1^{(1)} \\ \Delta x_2^{(1)} \\ \Delta x_1^{(2)} \\ \Delta x_2^{(2)} \end{pmatrix} = \begin{pmatrix} F_{1,1}^{(1)} & F_{1,2}^{(1)} & F_{1,3}^{(1)} \\ F_{2,1}^{(1)} & F_{2,2}^{(1)} & F_{2,3}^{(1)} \\ F_{1,1}^{(2)} & F_{1,2}^{(2)} & F_{1,3}^{(2)} \\ F_{2,1}^{(2)} & F_{2,2}^{(2)} & F_{2,3}^{(2)} \end{pmatrix} \begin{pmatrix} \Delta x_1 \\ \Delta x_2 \\ \Delta x_3 \end{pmatrix} \tag{1}$$

The three reconstructed components of the phase-averaged absolute velocity in the objective plane are shown in the Fig. 3 at three typical planes of the flow field.

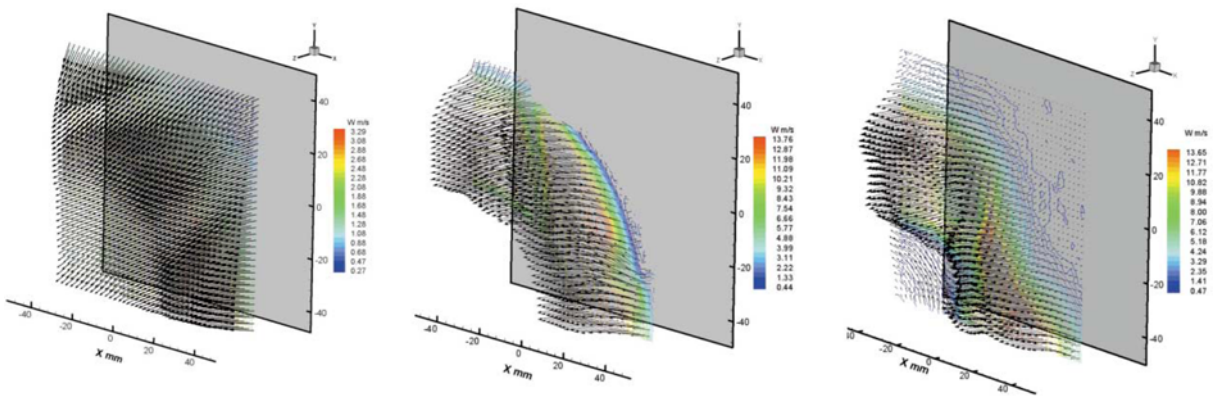

(a) Inlet (z/R = –1.75) (b) Internal (z/R = 0.13) (c) Outlet (z/R = 0.5)

Fig. 3. Reconstructed three components of velocity vectors.

In the present study, phase-averaged velocity fields were calculated based on 200 frames of the instantaneous stereoscopic PIV measurement results. In the inlet region ($z/R = -1.75$), it can be seen that ambient flow is induced toward the mid-span of the fan blades. From the view of phase-averaged velocity fields of inlet region, the flow pattern is more uniform and stable.

Figure 4 shows the stereoscopic PIV measurement results at two typical planes of the internal flow field. In order to reveal the cross stream in the selected locations clearly, the projections of the three-dimensional velocity vector in the cross planes (X-Y plane views) are presented in the figures. The test fan is rotating in the counter-clockwise direction and the x, y and z-axes are non-dimensionalized by the hub radius R. This figure represents the phase-averaged absolute velocity field at the $z/R = 0.13$ cross plane. The region of sudden decrease and direction change in velocity behind the blade spacing between two adjacent blades indicates the fan blade wake, of which the right side corresponds to the pressure side and the other suction side. High magnitude of velocity shows the presence of the leading edge where centrifugal force acts on fluid more strongly. Behind the blade tip, large depression of velocity and rolling up region toward the counterrotating direction appear where a large scale vortex can be noticed from radial velocity distribution. When the downstream distance increases to $z/R = 0.5$ the overall flow structure is observed to rotate about 15° in the counter-clockwise direction plane with a small overall decay in magnitude.

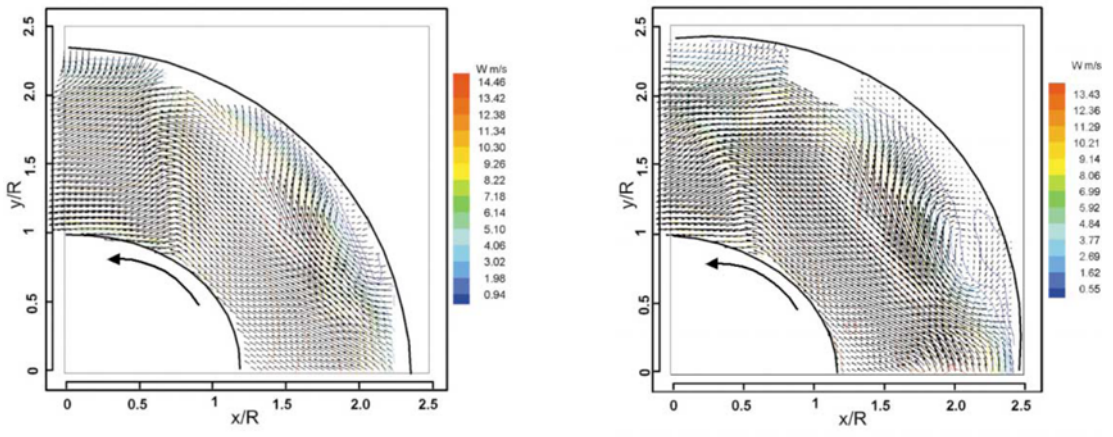

(a) z/R = 0.13 (b) z/R = 0.5

Fig. 4. Phase-averaged velocity (Internal).

Figure 5 shows the streamwise vorticity distribution calculated from the phase-averaged velocity data. Solid line represents positive (counter-clockwise) vortices and dashed lines represent negative clockwise vortices. At the cross plane $z/R = 0.13$, the negative vortices located along the blade tip. This is leakage vortex mainly due to rolling-up of tip leakage flow near the casing. Trailing vortex having high level of positive vorticity, which is ranged from near the hub to mid-span of the fan blade is observed with a single glance. In the $z/R = 0.5$ cross plane,

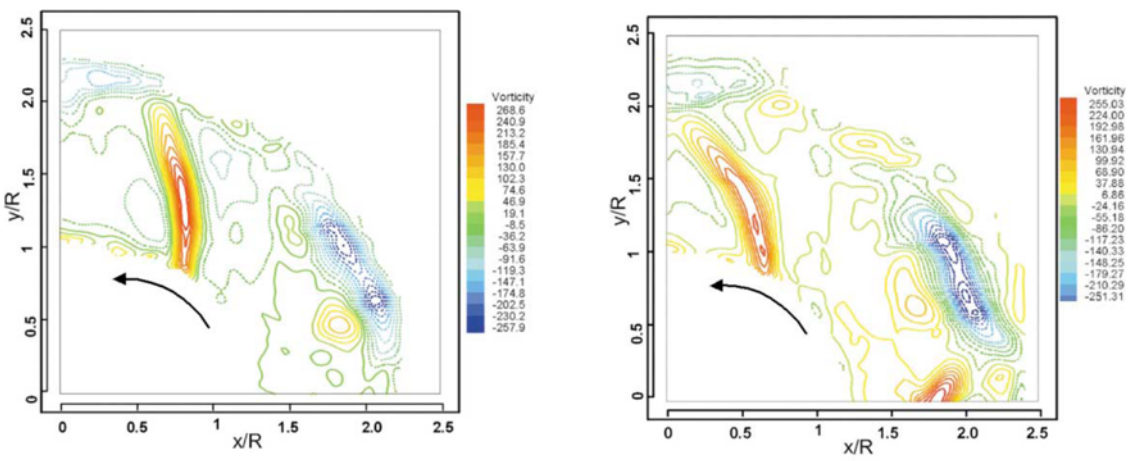

(a) z/R = 0.13 (b) z/R = 0.5

Fig. 5. Streamwise vorticity distribution (Internal).

the angular distance of vortices is changed comparing to that in the z/R = 0.13. The leakage vortex and trailing vortex keep the same structure with the magnitude reduction. All of the vorticity components show very high values behind the blade. However, trailing vortex has a higher decay ratio compared to the leakage vortex. The reason for that is the leakage vortex shedding into the flow with high energy due to the leakage jet flow by blade tip before rolling up.

At the z/R = 1.5 cross plane of the outlet flow field (Fig. 6), the effect of the presence of the rotor hub and the housing-support pole is exhibited by the low and negative velocity region. These negative velocity components, which may be caused by separation from hub cutting edgy, still can be found to the downstream about z/R = 2.0 (Fig. 7). The regions of high velocity near the blade tip and the low velocity near the root of the fan blade and associated flow pattern can be seen from the phase-average velocity. It means that this type of axial fan is designed to transfer energy to cooling air mainly with the blade tip rather the root of the fan.

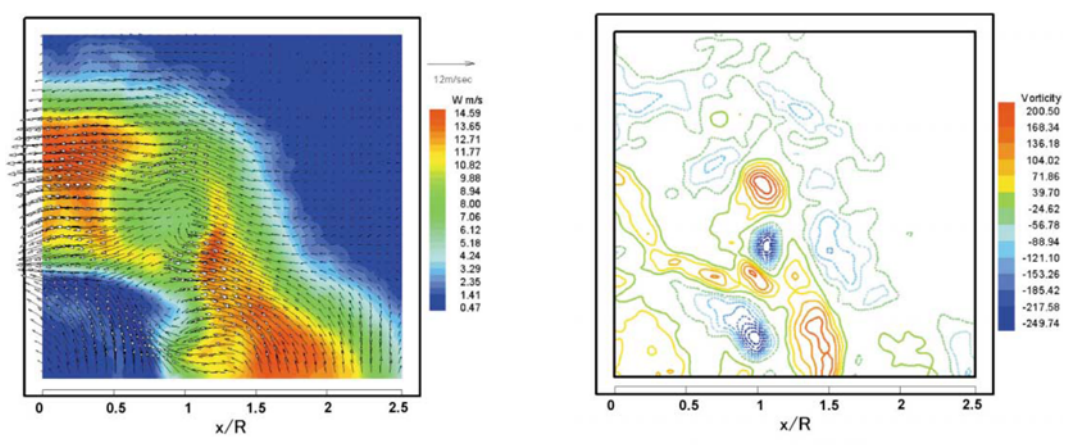

(a) Phase-averaged velocity (b) Vorticity distribution

Fig. 6. z/R= 1.5 (Outlet).

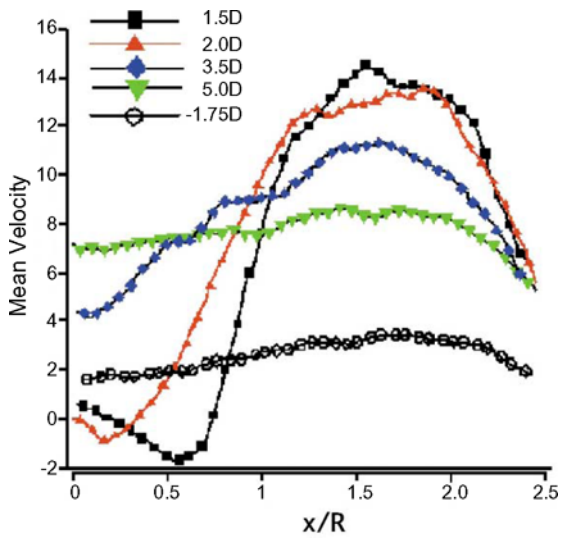

Fig. 7. Mean velocity profile.

Figures 8 and 9 show three-dimensional phase-averaged velocity iso-surface with the viewpoint from upstream and downstream. These were based on the stereoscopic PIV measurement results at 10 cross planes in total at the fields of internal and outlet side of the test fan ($0.13 < z/R < 5.0$). The velocity magnitudes of this iso-surface are ranged from −0.25 m/s (negative velocity region on the rotor boss) to 13.4 m/s (high speed velocity around tip blade) by changing the color from blue to red. From the reconstructed three-dimensional phase-averaged velocity iso-surface, the three-dimensional flow mechanism can be seen clearly. Large-scale streamwise vorticies, which may be another contributor to broadband noise generation, were mainly found along the hub edge and pole in this region.

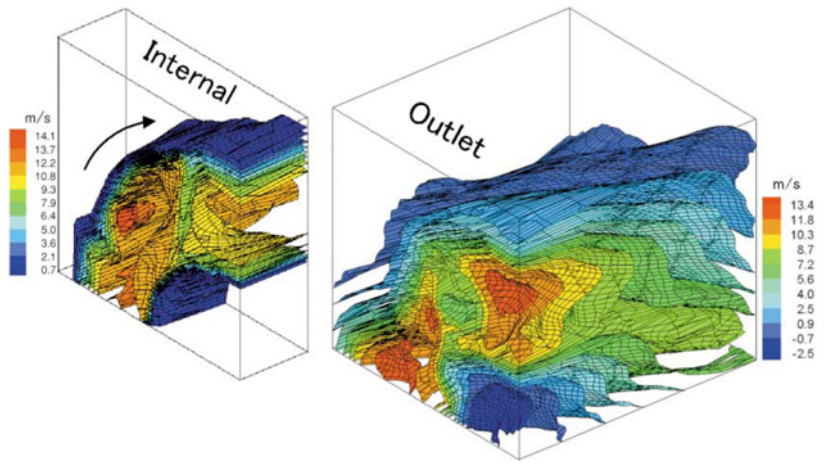

Fig. 8. Iso-surface velocity contour view from upsteam.

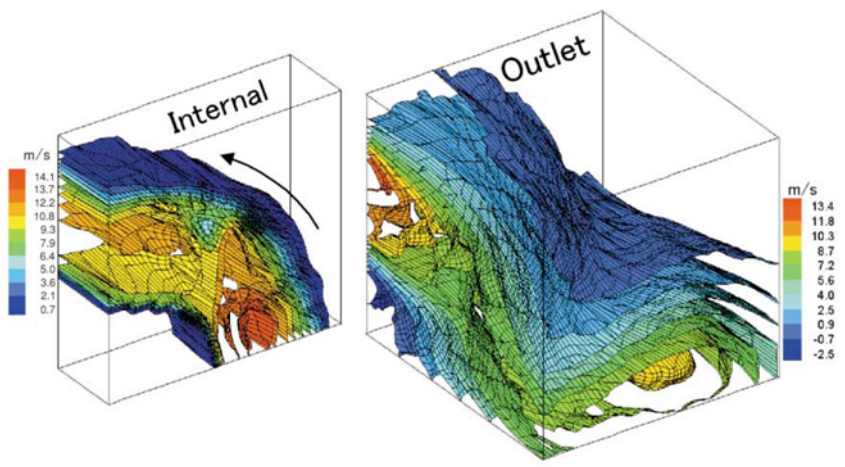

Fig. 9. Iso-surface velocity contour view from downstream.

4. Conclusion

The sterocsopic PIV system was used to conduct three-dimensional velocity measurement of inlet, internal and outlet sides of the axial flow fan. By the use of these measurement techniques, it is possible to elucidate quantitatively the three-dimensional structure of various kinds of vortices generated behind the blade.

The existence of large scale vortices caused by the fan blade orientation is revealed from PIV measurement result. Based on the result of the present experimental research, internal flow of the fan in relation to the mechanisms of vortical flows around the tip blade acting as a major source of noise, will be conducted in the coming work.

References

Adrian, R. J., Particle-image Techniques for Experimental Fluid Mechanic, Annual Review of Fluid Mechanics, (1991), 261.

Rajan, K. M., Wing T. L., Steve, D. H. and Tim, P. M., Measurement of Rotating Machinery Flows under Steady and Transient Operating Conditions using LDV and PIV, Proceedings of 9th ISALTFM, Lisbon (1998).

Saga, T., Three Dimensional Particle Image Velocimetry, The Textbook of the Seminar of Three-dimensional PIV, VSJ-PIV-S2. (ISBN4-906497-21-9), Yokohama, Japan (1999), 41.

Sharland, I. J., Source of Noise in Axial Flow Fans, J. Sound & Vibration 1-3, (1964), 302.

Author Profile

Im Yu Cheong: He received his bachelor degree in the Department of Mechanical Engineering from Korea Maritime University in 2000. He is a Master's student in Mechanical Engineering Department, the University of Tokyo. His research work mainly focused on experimental fluid mechanics with three-dimensional particle image velocimetry.

Tetsuo Saga: He graduated from Japan University in 1966 and he is a research associate in the Institute of Industrial Science, the University of Tokyo. His main research field is mechanical engineering. His research interests include flow visualization and its image analysis, prediction and control of flow induced vibration and automobile aerodynamics. Recently, he has interests in micro flow and bio flow analysis using PIV.

Toshio Kobayashi: He received his Ph.D. in the Mechanical Engineering Department, at the University of Tokyo in 1970. After completion of his Ph.D. program, he has been a faculty member of the Institute of Industrial Science (IIS), the University of Tokyo, and currently is a professor. His research interests are numerical analysis of turbulence, especially Large Eddy Simulation, and Particle Image Velocimetry. He serves as the President of the Visualization Society of Japan (VSJ), Executive Vice President of Automotive Engineers of Japan (JSAE) and President of the Japan Society of Mechanical Engineers (JSME).

Takahiro Ito: He graduated from Tsukuba University in 1982 and he is an engineer of Oriental Motor Co., Ltd. He is an expert on the wing design of fan. His main theme is developing low noise fans. For that purpose he is trying to make analysis by use of CFD (Computational Fluid Dynamics).